PHYSICAL REVIEW D **78**, 035015 (2008)

Dark matter constraints on the left-right symmetric model with Z_2 symmetry

Wan-lei Guo,* Li-ming Wang,+ Yue-liang Wu,‡ and Ci Zhuang§

Kavli Institute for Theoretical Physics China, Institute of Theoretical Physics, Chinese Academy of Science, Beijing 100080, People's Republic of China

(Received 12 May 2008; published 29 August 2008)

In the framework of the left-right symmetric model, we investigate an interesting scenario, in which the so-called vacuum expectation value (VEV)-seesaw problem can be naturally solved with Z_2 symmetry. In such a scenario, we find a pair of stable weakly interacting massive particles (WIMPs), which may be the cold dark matter candidates. However, the WIMP-nucleon cross section is 3–5 orders of magnitude above the present upper bounds from the direct dark matter detection experiments for $m \sim 10^2$–10^4 GeV. As a result, the relic number density of two stable particles has to be strongly suppressed to a very small level. Nevertheless, our analysis shows that this scenario cannot provide very large annihilation cross sections so as to give the desired relic abundance except for the resonance case. Only for the case if the rotation curves of disk galaxies are explained by the modified Newtonian dynamics (MOND), the stable WIMPs could be as the candidates of cold dark matter.

DOI: 10.1103/PhysRevD.78.035015 PACS numbers: 95.35.+d, 12.60.−i

I. INTRODUCTION

The left-right (LR) symmetric model [1], based on the gauge group $SU(2)_L \times SU(2)_R \times U(1)_{B-L}$, is an attractive extension of the standard model (SM). The symmetry requires the introduction of right-handed partners for the observed gauge bosons and neutrinos, and a Higgs sector containing one bidoublet ϕ (2, 2, 0), one left-handed triplet Δ_L (3, 1, 2), and one right-handed triplet Δ_R (1,3,2). In such a minimal LR symmetric model, parity is an exact symmetry of the theory at the high energy scale and is broken spontaneously at the low energy scale due to the asymmetric vacuum. Also CP asymmetry can be realized as a consequence of spontaneous symmetry breaking, namely, the spontaneous CP violation ($SCPV$) [2]. However, such a scenario suffers from nontrivial constraints from the vacuum minimization conditions. It is explicitly demonstrated that the $SCPV$ is not so easily realized if all the parameters in the Higgs potential are real and endowed with natural values [3–5]. The difficulty results from the facts that one of the neutral Higgs bosons carries a dangerous tree level flavor-changing neutral currents (FCNC) effect, and that quark flavor mixing angles and the CP violating phase are all calculable quantities due to the LR symmetry. Therefore, many generalized CP violation scenarios beyond the $SCPV$ case have been analyzed extensively [6–11]. In this literature, the masses of the right-handed gauge boson W_2 and the FCNC Higgs boson are strongly constrained from low energy phenomenology. Although the Cabibbo-Kobayashi-Maskawa (CKM) matrix are more general not to be fully fixed than the $SCPV$ case, it is proved that there is only one physical complex phase in the Yukawa couplings [12]. Hence the FCNC Higgs boson's couplings cannot be absolutely free. The FCNC Higgs boson's mass still accepts a strict bound. In terms of these observations, a generalized two Higgs bidoublet model is proposed [13]. In this model, quark mass matrices become far more flexible and the FCNC Higgs boson's Yukawa couplings are now free parameters. Thereby the low energy bound on the right-handed scale is largely alleviated. As other generalized models, the two Higgs bidoublet version of the LR model also has the advantage to realize the $SCPV$ without the fine-tuning problem.

The LR symmetric model is also motivated to explain the very tiny neutrino masses. When the vacuum expectation value (VEV) v_R of the neutral component of Δ_R is very huge, typically of order 10^{12} GeV, the well-known seesaw mechanism provides a very natural explanation of the smallness of neutrino masses [14]. However, the right-handed gauge bosons Z_2 and W_2 are too heavy to be detected at the Large Hadron Collider (LHC) and the future colliders. To allow for the possibility of an observable right-handed scale, many authors focus on the $v_R \sim$ 10 TeV case. Although the seesaw mechanism can work well, we have to face the so-called VEV-seesaw puzzle. Namely, β/ρ is of order 10^{-10} rather than the anticipant $\mathcal{O}(1)$, where ρ and β are located in the Higgs potential. One may introduce a discrete Z_2 symmetry $\Delta_L \to -\Delta_L$ and $\Delta_R \to \Delta_R$ to resolve this VEV-seesaw problem [4]. It is worthwhile to stress that neutrinos are the Dirac particles in this scenario. If we preserve the Majorana Yukawa couplings, the corresponding model must lie beyond the LR symmetric model.

The Z_2 symmetry leads to the absence of both β-type terms and the Majorana Yukawa couplings, hence $v_L = 0$ due to the minimization conditions. Furthermore, we find that the neutral Higgs bosons δ_L^0 and δ_L^{0*} are a pair of stable

*guowl@itp.ac.cn
+wanglm@itp.ac.cn
‡ylwu@itp.ac.cn
§zhuangc@itp.ac.cn

weakly interacting massive particles (WIMPs). This is an important feature of our scenario which has not been indicated before. It is a natural idea that δ_L^0 and δ_L^{0*} may be the cold dark matter candidates [15]. We first calculate the WIMP-nucleon elastic scattering cross section which has been strongly constrained by the direct dark matter detection experiments, such as the CDMS [16] and XENON [17]. However, our result is 3–5 orders of magnitude above the present bounds for $m \sim 10^2$–10^4 GeV [16,17]. To avoid this puzzle, δ_L^0 and δ_L^{0*} cannot dominate all the dark matter. We find that our scenario is consistent with the direct dark matter detection experiments only when $n_{\delta_L^0} \leq 4.8 \times 10^{-14}$, where $n_{\delta_L^0}$ is the total relic number density of δ_L^0 and δ_L^{0*}. This bound requires that the dark matter annihilation cross sections must be very large. In this work, we examine whether our scenario can provide very large annihilation cross sections so as to derive the desired relic abundance.

In this paper we try to give a comprehensive analysis on these LR models with general parameter setting. First, we perform a detailed investigation on the simplest LR model with one Higgs bidoublet, in which there are not any *CP* violation phases. Then we generalize the simplest LR model to some other more complicated situations. It turns out that there is no significant differences among these one Higgs bidoublet versions of the LR model because the gauge and Higgs sectors are basically the same. Whereas in the two Higgs bidoublet case, there would be more Higgs bosons and the Yukawa couplings might be quite different. Hence more delicate analysis is needed. The remaining part of this paper is organized as follows. In Sec. II, we briefly describe the main features of the LR symmetric model and discuss the VEV-seesaw problem. In Secs. III and IV the direct dark matter detection experiments put very strong constraints on the relic number density and the annihilation cross sections. In Sec. V, we analyze whether the simplest LR model can be consistent with the above constraints or not. Then we generalize the simplest LR model to the two Higgs bidoublets case in Sec. VI. The summary and comments are given in Sec. VII.

II. THE LR SYMMETRIC MODEL WITH Z_2 SYMMETRY

The minimal LR symmetric model consists of one Higgs bidoublet ϕ (2, 2, 0), one left-handed Higgs triplet Δ_L (3, 1, 2), and one right-handed Higgs triplet Δ_R (1, 3, 2), which can be written as

$$\phi = \begin{pmatrix} \phi_1^0 & \phi_1^+ \\ \phi_2^- & \phi_2^0 \end{pmatrix}; \qquad \Delta_{L,R} = \begin{pmatrix} \delta_{L,R}^+/\sqrt{2} & \delta_{L,R}^{++} \\ \delta_{L,R}^0 & -\delta_{L,R}^+/\sqrt{2} \end{pmatrix}. \tag{1}$$

After the spontaneous symmetry breaking, the Higgs multiplets can have the following vacuum expectation values:

$$\langle\phi\rangle = \begin{pmatrix} \kappa_1/\sqrt{2} & 0 \\ 0 & \kappa_2/\sqrt{2} \end{pmatrix}; \qquad \langle\Delta_{L,R}\rangle = \begin{pmatrix} 0 & 0 \\ v_{L,R}/\sqrt{2} & 0 \end{pmatrix}, \tag{2}$$

where κ_1, κ_2, v_L, and v_R are in general complex. Without loss of generality, one can choose κ_1 and v_R to be real, while assigning complex phases θ_2 and θ_L for κ_2 and v_L, respectively. Following the requirements of the LR symmetry, we can write down the most general form of the Higgs potential [4]

$$\begin{aligned} V = {}& -\mu_1^2(\mathrm{Tr}[\phi^\dagger\phi]) - \mu_2^2(\mathrm{Tr}[\tilde{\phi}\phi^\dagger] + \mathrm{Tr}[\tilde{\phi}^\dagger\phi]) - \mu_3^2(\mathrm{Tr}[\Delta_L\Delta_L^\dagger] + \mathrm{Tr}[\Delta_R\Delta_R^\dagger]) + \lambda_1((\mathrm{Tr}[\phi\phi^\dagger])^2) + \lambda_2((\mathrm{Tr}[\tilde{\phi}\phi^\dagger])^2 \\ & + (\mathrm{Tr}[\tilde{\phi}^\dagger\phi])^2) + \lambda_3(\mathrm{Tr}[\tilde{\phi}\phi^\dagger]\mathrm{Tr}[\tilde{\phi}^\dagger\phi]) + \lambda_4(\mathrm{Tr}[\phi\phi^\dagger](\mathrm{Tr}[\tilde{\phi}\phi^\dagger] + \mathrm{Tr}[\tilde{\phi}^\dagger\phi])) + \rho_1((\mathrm{Tr}[\Delta_L\Delta_L^\dagger])^2 \\ & + (\mathrm{Tr}[\Delta_R\Delta_R^\dagger])^2) + \rho_2(\mathrm{Tr}[\Delta_L\Delta_L]\mathrm{Tr}[\Delta_L^\dagger\Delta_L^\dagger] + \mathrm{Tr}[\Delta_R\Delta_R]\mathrm{Tr}[\Delta_R^\dagger\Delta_R^\dagger]) + \rho_3(\mathrm{Tr}[\Delta_L\Delta_L^\dagger]\mathrm{Tr}[\Delta_R\Delta_R^\dagger]) \\ & + \rho_4(\mathrm{Tr}[\Delta_L\Delta_L]\mathrm{Tr}[\Delta_R^\dagger\Delta_R^\dagger] + \mathrm{Tr}[\Delta_L^\dagger\Delta_L^\dagger]\mathrm{Tr}[\Delta_R\Delta_R]) + \alpha_1(\mathrm{Tr}[\phi\phi^\dagger](\mathrm{Tr}[\Delta_L\Delta_L^\dagger] + \mathrm{Tr}[\Delta_R\Delta_R^\dagger])) \\ & + \alpha_2(\mathrm{Tr}[\phi\tilde{\phi}^\dagger]\mathrm{Tr}[\Delta_R\Delta_R^\dagger] + \mathrm{Tr}[\phi^\dagger\tilde{\phi}]\mathrm{Tr}[\Delta_L\Delta_L^\dagger]) + \alpha_2^*(\mathrm{Tr}[\phi^\dagger\tilde{\phi}]\mathrm{Tr}[\Delta_R\Delta_R^\dagger] + \mathrm{Tr}[\tilde{\phi}^\dagger\phi]\mathrm{Tr}[\Delta_L\Delta_L^\dagger]) \\ & + \alpha_3(\mathrm{Tr}[\phi\phi^\dagger\Delta_L\Delta_L^\dagger] + \mathrm{Tr}[\phi^\dagger\phi\Delta_R\Delta_R^\dagger]) + \beta_1(\mathrm{Tr}[\phi\Delta_R\phi^\dagger\Delta_L^\dagger] + \mathrm{Tr}[\phi^\dagger\Delta_L\phi\Delta_R^\dagger]) + \beta_2(\mathrm{Tr}[\tilde{\phi}\Delta_R\phi^\dagger\Delta_L^\dagger] \\ & + \mathrm{Tr}[\tilde{\phi}^\dagger\Delta_L\phi\Delta_R^\dagger]) + \beta_3(\mathrm{Tr}[\phi\Delta_R\tilde{\phi}^\dagger\Delta_L^\dagger] + \mathrm{Tr}[\phi^\dagger\Delta_L\tilde{\phi}\Delta_R^\dagger]), \end{aligned} \tag{3}$$

where $\tilde{\phi} = \tau_2\phi^*\tau_2$ and all parameters μ_i, λ_i, ρ_i, α_i, and β_i are real. Only α_2 can be complex. The phases of κ_2 and v_L may lead to the *SCPV* [2]. It has been shown that the combing constraints from the K and B system actually exclude the minimal LR symmetric model with the *SCPV* in the decoupling limit [9]. For our present purpose, we investigate here the simplest LR model, in which α_2, κ_2, v_L, and the Yukawa couplings are real. It is worthwhile to stress that our remaining analysis can be generalized to the other *CP* violation scenarios [6–11].

In the minimal LR symmetric model, the Lagrangian relevant for the neutrino masses reads [4]:

$$\begin{aligned} -\mathcal{L} = {}& Y_\nu\bar{\psi}_L\phi\psi_R + \tilde{Y}_\nu\bar{\psi}_L\tilde{\phi}\psi_R + Y_M(\bar{\psi}_L^c i\tau_2\Delta_L\psi_L \\ & + \bar{\psi}_R^c i\tau_2\Delta_R\psi_R) + \mathrm{H.c.}, \end{aligned} \tag{4}$$

where $\psi_{L,R} = (\nu_{L,R}, l_{L,R})^T$. After the spontaneous symmetry breaking, one may obtain the effective (light and left-handed) neutrino mass matrix m_ν via the type II seesaw mechanism:

$$m_\nu = \sqrt{2}\left(Y_M v_L - \frac{Y_D^2 \kappa^2}{2Y_M v_R}\right), \quad (5)$$

where $\kappa = \sqrt{|\kappa_1|^2 + |\kappa_2|^2} \approx 246$ GeV represents the electroweak symmetry breaking (EWSB) scale and $Y_D = (Y_\nu \kappa_1 + \tilde{Y}_\nu \kappa_2)/(\sqrt{2}\kappa)$. The charged lepton mass matrix is given by $m_l = (Y_\nu \kappa_2 + \tilde{Y}_\nu \kappa_1)/\sqrt{2}$. The electroweak precision test requires $v_L \ll \kappa$. Barring extreme fine-tuning, the neutrino masses $m_\nu \sim 0.1$ eV [18] force v_L to be of order a few eV or less, thereby requiring $v_R \sim 10^{12}$ GeV for $Y_D \sim Y_M \sim m_l/\kappa$. In this case, the right-handed gauge bosons Z_2 and W_2 are too heavy to be detected at the LHC and the future colliders. To allow for the possibility of an observable right-handed scale, many authors focus on the $v_R \sim 10$ TeV case. Although the seesaw mechanism can work well, we need to resolve the so-called VEV-seesaw puzzle [4], which is indicated by a simple vacuum minimization equation:

$$(2\rho_1 - \rho_3) v_L v_R = \beta_1 \kappa_1 \kappa_2 + \beta_2 \kappa_1^2 + \beta_3 \kappa_2^2. \quad (6)$$

Without loss of generality, one can write Eq. (6) in a compact form:

$$\gamma \equiv \frac{\beta}{\rho} = \frac{v_L v_R}{\kappa^2}. \quad (7)$$

In view of the naturalness, one expects $\gamma \sim \mathcal{O}(1)$. However, we find that $\gamma \sim 10^{-10}$ as long as $v_R \sim 10$ TeV. This is the infamous VEV-seesaw problem in the literature [4]. The neutrino mass matrix m_ν in Eq. (5) can also be written as

$$m_\nu = \sqrt{2}\left(Y_M \gamma - \frac{Y_D^2}{2Y_M}\right)\frac{\kappa^2}{v_R}. \quad (8)$$

It is shown that the VEV-seesaw relationship implies the unnaturalness for the auxiliary parameter γ if one wants to search for new physics at the TeV scale. To avoid the VEV-seesaw puzzle, a smart way is to introduce some new symmetries to eliminate all β-type terms of the Higgs potential. However this is not an easy task in the current model. One may guess there exists some additional global symmetries like $U(1)$ acting on the Higgs fields which can eliminate all β-type terms [4]. However, such an alternative always affects the fermion sector and fails to give correct fermion masses and mixing. If there is an approximate $U(1)$ horizontal symmetry to suppress β_i without eliminating them completely, then one may solve the VEV-seesaw problem [10,19]. Unfortunately, this model yields a small mixing angle within the first two lepton generations. In Ref. [4], the authors suggest a Z_2 symmetry

$$\Delta_L \to -\Delta_L, \qquad \Delta_R \to \Delta_R, \quad (9)$$

which can eliminate all β-type terms of the Higgs potential. However, this discrete symmetry also eliminates the Majorana Yukawa couplings, which implies that neutrinos are Dirac particles. At this moment, Eq. (6) becomes

$$(2\rho_1 - \rho_3) v_L = 0. \quad (10)$$

One may immediately dismiss the possibility $2\rho_1 - \rho_3 = 0$, which implies two massless left-handed Higgs triplet bosons. Thus the only left choice is $v_L = 0$. The Z_2 symmetry leads to $v_L = 0$ and the absence of both β-type terms and Majorana Yukawa couplings. Furthermore, we find that the lightest particles among the members of the left-handed Higgs triplet Δ_L, namely δ_L^0 and δ_L^{0*}, are two degenerate and stable particles. A natural idea is that δ_L^0 and δ_L^{0*} may be the cold dark matter candidates. In the following sections we shall discuss the possibility of δ_L^0 and δ_L^{0*} being the cold dark matter candidates by evaluating all relevant annihilation processes. The main features of the LR symmetric model with Z_2 symmetry have been shown in Ref. [20]. Here, we show the mass spectrum for the Higgs bosons and gauged bosons at leading order in Table I, with approximations $\kappa^2/v_R^2 \simeq 0$ and $\kappa_2/\kappa_1 \simeq 0$ mentioned in the appendix. Gauge bosons Z_1 and Z_2 are defined by $Z_1 = c_W W_{3L} - s_W t_W W_{3R} - \sqrt{c_{2W}} t_W B$ and $Z_2 = \sqrt{c_{2W}} \sec_W W_{3R} - t_W B$, where the subscript W denotes the Weinberg angle θ_W. In addition, all the trilinear and quartic scalar interactions and scalar-gauge interactions are listed in the appendix for convenience.

TABLE I. The mass spectrum for the Higgs bosons and the gauged bosons in the LR symmetric model with Z_2 symmetry. Here, we have neglected the terms in order of κ_2/κ_1 and κ^2/v_R^2.

Particles	Mass^2	Particles	Mass^2
$h^0 = \phi_1^{0r}$	$m_{h^0}^2 = 2\lambda_1 \kappa^2$	$H_1^\pm = \phi_1^\pm$	$m_{H_1^\pm}^2 = \frac{1}{2}\alpha_3(v_R^2 + \frac{1}{2}\kappa^2)$
$H_1^0 = \phi_2^{0r}$	$m_{H_1^0}^2 = \frac{1}{2}\alpha_3 v_R^2 + 2\kappa^2(2\lambda_2 + \lambda_3)$	$\delta_R^{\pm\pm}$	$m_{\delta_R^{\pm\pm}}^2 = 2\rho_2 v_R^2 + \frac{1}{2}\alpha_3\kappa^2$
$A_1^0 = -\phi_2^{0i}$	$m_{A_1^0}^2 = \frac{1}{2}\alpha_3 v_R^2 - 2\kappa^2(2\lambda_2 - \lambda_3)$	$\delta_L^\pm$	$m_{\delta_L^\pm}^2 = \frac{1}{2}(\rho_3 - 2\rho_1)v_R^2 + \frac{1}{4}\alpha_3\kappa^2$
$H_2^0 = \delta_R^{0r}$	$m_{H_2^0}^2 = 2\rho_1 v_R^2$	$\delta_L^{\pm\pm}$	$m_{\delta_L^{\pm\pm}}^2 = \frac{1}{2}(\rho_3 - 2\rho_1)v_R^2 + \alpha_3\kappa^2$
δ_L^0, δ_L^{0*}	$m^2 = \frac{1}{2}(\rho_3 - 2\rho_1)v_R^2$		
Z_1	$m_{Z_1}^2 = \frac{g^2\kappa^2}{4\cos^2\theta_W}$	$W_1^\pm = W_L^\pm$	$m_{W_1}^2 = \frac{g^2\kappa^2}{4}$
Z_2	$m_{Z_2}^2 = \frac{g^2 v_R^2 \cos^2\theta_W}{\cos 2\theta_W}$	$W_2^\pm = W_R^\pm$	$m_{W_2}^2 = \frac{g^2 v_R^2}{2}$

III. THE DIRECT DARK MATTER DETECTION

The current direct dark matter detection experiments, such as the CDMS [16] and XENON [17], have provided very strong constraints on the WIMP-nucleus elastic cross section. The rate for direct detection of dark matter candidates is given by [15]

$$R \approx \sum_i N_i \frac{\rho_{\rm local}}{m} \langle \sigma_{i\mathcal{N}} \rangle, \tag{11}$$

where N_i is the number of nuclei with species i in the detector, $\rho_{\rm local}$ is the local energy density of dark matter, and m is the mass of cold dark matter. $\sigma_{i\mathcal{N}}$ is the WIMP-nucleus elastic cross section, and the angular brackets denote an average over the relative WIMP velocity with respect to the detector. Using the standard assumptions of $\rho_{\rm local}$ and distribution of the relative WIMP velocity [21], one can derive the constrains on the WIMP-nucleon cross section $\sigma_n^{\rm exp} \le 4.6 \times 10^{-44}$ cm^2 for $m = 60$ GeV from the CDMS [16]; $\sigma_n^{\rm exp} \le 8.8 \times 10^{-44}$ cm^2 for $m = 100$ GeV from the XENON [17]. Since the WIMP flux decreases $\propto 1/m$, $\sigma_n^{\rm exp} \propto m$ is a very good assumption for $m > 100$ GeV.

In our scenario, the dark matter candidates δ_L^0 and δ_L^{0*} interact with nucleus $\mathcal{N}$ through their couplings with quarks by exchanging the neutral gauge bosons Z_1, Z_2, and Higgs bosons. We find that the main contribution comes from the Z_1 exchanging process, which produces a spin-independent elastic cross section on a nucleus $\mathcal{N}$ [22]

$$\sigma_{\mathcal{N}} = \frac{2G_F^2 M^2(\mathcal{N})}{\pi}[(A - Z) - (1 - 4\sin^2\theta_W)Z]^2, \tag{12}$$

where Z and $A - Z$ are the numbers of protons and neutrons in the nucleus, respectively. G_F is the Fermi coupling constant and $M(\mathcal{N}) = mM_{\mathcal{N}}/(m + M_{\mathcal{N}})$ is the reduced WIMP mass. Traditionally, the results of WIMP-nucleus elastic experiments are presented in the form of a normalized WIMP-nucleon cross section σ_n in the spin-independent case, which is straightforward

$$\sigma_n = \frac{1}{A^2} \frac{M^2(n)}{M^2(\mathcal{N})} \sigma_{\mathcal{N}}, \tag{13}$$

where $M(n) = mM_n/(m + M_n)$ and M_n denotes the nucleon mass. When $m \gg M_n$, one may arrive at $\sigma_n = 8.2 \times 10^{-39}$ cm^2 for the CDMS experiment, which is 3–5 orders of magnitude above the present bounds for $m \sim 10^2$–10^4 GeV [17]. Therefore, such dark matter candidates are excluded by the current direct detection experiments.

If δ_L^0 and δ_L^{0*} have a nonzero splitting, one can avoid the above bounds since the Z_1 exchanging process is forbidden kinematically [23]. However, such degeneracy cannot be satisfied in our model. If the energy density of δ_L^0 and δ_L^{0*} in the solar system is far less than $\rho_{\rm local}$, we can avoid the above experimental limits as shown in Eq. (11). This means that δ_L^0 and δ_L^{0*} are only a very small part of the total dark matter. We find that our model is consistent with the direct detection experiments only when

$$n_{\delta_L^0} \le 4.8 \times 10^{-14}, \tag{14}$$

where $n_{\delta_L^0}$ is the total relic number density of δ_L^0 and δ_L^{0*}. Here we have taken the approximation $\sigma_n^{\rm exp} \propto m$ (when $m \ge 100$ GeV) and used $\sigma_n^{\rm exp} = 3.4 \times 10^{-43}$ cm^2 ($m = 1$ TeV) as the input parameter [16]. It is worthwhile to stress that the bound in Eq. (14) is not valid for $m < 100$ GeV.

The present experimental bounds are based on the standard assumptions for the galactic halo [21]. It needs to be mentioned that the rotation curves of disk galaxies may also be explained by the modified Newtonian dynamics (MOND) [24]. On one hand, we use the MOND to account for the rotation curve of the Milky Way; on the other hand, we still believe that the cold dark matter exists in the Universe. In this case, the local energy density of cold dark matter may be far less than the standard assumption. Therefore, we may give up the above constraints from the direct dark matter detection experiments. Subsequently, the stable particles δ_L^0 and δ_L^{0*} may be the cold dark matter.

IV. CONSTRAINTS ON THE ANNIHILATION CROSS SECTION

The thermal average of the annihilation cross section times the "relative velocity" $\langle \sigma v \rangle$ is a key quantity in the determination of the cosmic relic abundances of δ_L^0 and δ_L^{0*}. The constraint in Eq. (14) implies $\langle \sigma v \rangle$ must be very large in our scenario. In this section, we analyze whether the present model can satisfy Eq. (14).

In our scenario, δ_L^i ($i = 1, \ldots, 6$ for δ_L^0, δ_L^{0*}, $\delta_L^{\pm}$, and $\delta_L^{\pm\pm}$) are a set of similar particles whose masses may be nearly degenerate. The total relic density of the lightest particles δ_L^0 and δ_L^{0*} is determined not only by their annihilation cross sections, but also by the annihilation of the heavier particles, which will later decay into δ_L^0 or δ_L^{0*}. Therefore, we need to consider the coannihilation processes [25]. Since $\delta_L^{\pm}$ and $\delta_L^{\pm\pm}$ which survive annihilation eventually decay into δ_L^0 or δ_L^{0*}, the relevant quantity is the total number density of δ_L^i, $n = \sum_{i=1}^6 n_i$. The evolution of n is given by the following Boltzmann equation [25]:

$$\frac{dn}{dt} = -3Hn - \langle \sigma_{\rm eff} v \rangle (n^2 - n_{\rm eq}^2), \tag{15}$$

where H is the Hubble parameter, $n_{\rm eq}$ is the total equilibrium number density, and v is the relative velocity of two annihilation particles. The effective annihilation cross section $\sigma_{\rm eff}$ is

$$\sigma_{\rm eff} = \sum_{ij}^{6} \sigma_{ij} \frac{g_i g_j}{g_{\rm eff}^2} (1 + \Delta_i)^{3/2} (1 + \Delta_j)^{3/2} e^{-x(\Delta_i + \Delta_j)}, \tag{16}$$

where $\Delta_i = (m_i - m)/m$, $x \equiv m/T$ is the scaled inverse temperature. $g_i = 1$ is the internal degrees of freedom of δ_L^i and $g_{\rm eff} = \sum_{i=1}^6 g_i(1+\Delta_i)^{3/2}e^{-x\Delta_i}$. For the total equilibrium number density, we may use the nonrelativistic approximation $n_{\rm eq} \approx g_{\rm eff}(mT/2\pi)^{3/2}\exp(-m/T)$.

For particles which potentially play the role of cold dark matter, the relevant freeze-out temperature is $x_f = m/T \sim 25$. In our scenario, one can derive $x_f \gtrsim 35$ which can be seen in Eq. (19). When $\Delta_i > 0.1$ for $\delta_L^\pm$ and $\delta_L^{\pm\pm}$, we can arrive at $\sigma_{\rm eff} = \sigma_{12}/2$ in our model. In addition, we find that it is also a rational approximation $\sigma_{\rm eff} \approx \sigma_{12}/2$ even if all masses of δ_L^i are nearly degenerate. For simplicity, we take $\langle\sigma_{\rm eff}v\rangle = \langle\sigma_{12}v\rangle/2$ in the remaining analysis of our paper.

For nonrelativistic gases, the thermally averaged annihilation cross section $\langle\sigma_{12}v\rangle$ may be expanded in powers of x^{-1}, $\langle\sigma_{12}v\rangle = \sigma_0 x^{-k}$, $k=0$ for the s-wave annihilation and $k=1$ for the p-wave annihilation [26]. The general formula for $\langle\sigma_{12}v\rangle$ is given by [27]

$$\langle\sigma_{12}v\rangle = \sigma_0 x^{-k} = \frac{1}{m^2}\left[\omega - \frac{3}{2}(2\omega - \omega')x^{-1} + \ldots\right]_{s/4m^2=1}, \quad (17)$$

where $\omega \equiv E_1E_2\sigma_{12}v$, prime denotes derivative with respect to $s/4m^2$, and s is the center-of-mass squared energy. ω and its derivative are all to be evaluated at $s/4m^2 = 1$. The final number density $n_{\delta_L^0}$ is given by [26]

$$n_{\delta_L^0} = 2970\frac{3.79(k+1)x_f^{k+1}}{g_*^{1/2}M_{\rm Pl}m\sigma_0/2}\,{\rm cm}^{-3} \quad (18)$$

with

$$x_f = \ln[0.038(k+1)(g_{\rm eff}/g_*^{1/2})M_{\rm Pl}m\sigma_0/2] - (k+1/2) \times \ln\{\ln[0.038(k+1)(g_{\rm eff}/g_*^{1/2})M_{\rm Pl}m\sigma_0/2]\}, \quad (19)$$

where $M_{\rm Pl} = 1.22\times10^{19}$ GeV and g_* is the total number of effectively relativistic degrees of freedom at the time of freeze-out. Here we take $g_* \approx 100$ for illustration. With the help of Eqs. (14), (18), and (19), we can derive

$$m\sigma_0 \geq 0.13\ {\rm GeV}^{-1}\quad (s\text{-wave}); \qquad m\sigma_0 \geq 9.8\ {\rm GeV}^{-1}\quad (p\text{-wave}). \quad (20)$$

V. ONE HIGGS BIDOUBLET MODEL

In this section, we shall investigate whether the above bounds can be satisfied in one Higgs bidoublet model or not. Since there are many unknown parameters, some rational assumptions have to be made for our model so that one can calculate all relevant annihilation processes. In our scenario, the thermally averaged annihilation cross section $\langle\sigma_{12}v\rangle$ is usually inverse proportional to m^2 as shown in Eq. (17). Therefore, one can obtain $m\sigma_0 \propto 1/v_R$. Namely, the smaller v_R is, the easier Eq. (20) can be satisfied. Considering the constraints on the masses of W_2 and the FCNC Higgs boson from low energy phenomenology [11], we choose $v_R = 10$ TeV and $\alpha_3 = 2$ as an instructive example to illustrate the main features of our scenario. One can immediately get $m_{Z_2} = 7.5$ TeV and $m_{W_2} = 4.5$ TeV. Now let us introduce an auxiliary parameter $\varepsilon \equiv (\rho_3 - 2\rho_1)/(2\rho_1)$ to reexpress the mass of δ_L^0 and δ_L^{0*}

$$m = \sqrt{\tfrac{1}{2}(\rho_3 - 2\rho_1)}v_R = \sqrt{\varepsilon\rho_1}v_R. \quad (21)$$

From the Z_1 invisible width one may obtain $m > m_{Z_1}/2$, which requires $\varepsilon\rho_1 > 2.0\times10^{-5}$. On the other hand, we may require $\rho_3 \leq 4$ in view of the perturbativity, and then derive $\rho_1 + \varepsilon\rho_1 \leq 2$. In addition, we wish all ρ_i have the same order which means $\varepsilon \leq 4$. Because of the suppression of phase space, one may ignore some annihilation processes in terms of the values of ε and ρ_1. When $m < m_{W_1}$, δ_L^0 and δ_L^{0*} mainly annihilate into the fermion pairs (except for top quark). The corresponding $m\sigma_0$ is far less than the lower bound of Eq. (20). For the convenience of the remaining analysis, we require $m \geq 500$ GeV (namely, $\varepsilon\rho_1 \geq 2.0\times10^{-3}$) which does not affect our conclusions. Finally, we assume that all α_i of the Higgs potential have the same order.

It is worthwhile to stress that Eq. (17) is not valid when the annihilation takes place near a pole in the cross section [25]. This happens, for example, in Z-exchange annihilation when the mass of relic particle is near $m_Z/2$. For the cases $2m/m_Z \leq 0.8$ and $2m/m_Z \geq 1.2$, we use the above analytic way to calculate $m\sigma_0$. On the contrary, we should numerically solve the Boltzmann equation in Eq. (15), in which the resonant cross sections of the Breit-Wigner form must be considered. Then one can derive the relic number density $n_{\delta_L^0}$ which has to be less than the upper bound in Eq. (14).

In general, all relevant annihilation processes may be divided into four categories in terms of the different final states: $\delta_L^0\delta_L^{0*} \to f\bar{f}$, $\delta_L^0\delta_L^{0*} \to VV$, $\delta_L^0\delta_L^{0*} \to HH$, and $\delta_L^0\delta_L^{0*} \to VH$, where V and H denote the gauge boson and the Higgs boson, respectively. Next, we shall analyze in detail the four classes of annihilation processes and the resonance case.

A. $\delta_L^0\delta_L^{0*} \to f\bar{f}$

Let us start with the first case: δ_L^0 and δ_L^{0*} annihilate into fermion pairs. There are two kinds of Feynman diagrams at the tree level contributing to this case: S channel gauge bosons exchanging and Higgs bosons exchanging diagrams. Because of the absence of Majorana-type Yukawa couplings, there are no T channel diagrams contribution. The first amplitude is proportional to e^2, while the second is proportional to $\alpha m_f/\sqrt{s}$. It is plausible that both diagrams have the same contribution for $m \sim 500$ GeV. However, the squared amplitude of the first diagram always includes a suppression factor of $1 - 4m^2/s$, which leads to the p-wave annihilation.

For the gauge bosons exchanging diagram, we can obtain

$$\omega_{f\bar{f}} \approx E_1 E_2 \sigma_{f\bar{f}} v \approx \frac{e^4}{4\pi}\left(1 - \frac{4m^2}{s}\right)\frac{9s^2 - 19m_{Z_2}^2 s + 11m_{Z_2}^4}{(s - m_{Z_2}^2)^2}. \tag{22}$$

It is obvious that this is a p-wave annihilation process. With the help of Eq. (17), we have $(m\sigma_0)_{f\bar{f}} \le 2.2 \times 10^{-5}\ \mathrm{GeV}^{-1}$ for $m \ge 500$ GeV. It is 6 orders less than the lower bound $m\sigma_0 \ge 9.8\ \mathrm{GeV}^{-1}$. Although one may increase $m\sigma_0$ through lowering m, $(m\sigma_0)_{f\bar{f}}$ is still far less than the lower bound in Eq. (20) even if $m = 100$ GeV. Therefore, this process cannot suppress the relic number density of δ_L^0 and δ_L^{0*}.

For the Higgs bosons exchanging diagram, the exchanged particles should be h^0 and H_1^0. As shown in Table I, the mass of H_1^0 is far more than the light SM Higgs mass m_{h^0}. Because of the suppression of the propagator, we neglect the contribution from H_1^0. For the h^0 case, the amplitude of the Higgs bosons exchanging process is proportional to m_f. Furthermore, we only consider the top quark pair final states. The relevant cross section is

$$\omega_{\mathrm{top}} \approx \frac{3}{16\pi}\frac{(\alpha_1 m_t)^2 s}{(s - m_{h^0}^2)^2}, \tag{23}$$

which leads to a s-wave annihilation process. One may immediately derive $(m\sigma_0)_{\mathrm{top}} \le 1.5 \times 10^{-5}\ \mathrm{GeV}^{-1}$ for $m \ge 500$ GeV and $\alpha_1 = 2$, which is far less than the lower bound $m\sigma_0 \ge 0.13\ \mathrm{GeV}^{-1}$.

B. $\delta_L^0 \delta_L^{0*} \to VV$

In Fig. 1, we show all possible Feynman diagrams for the process $\delta_L^0 \delta_L^{0*} \to VV$. There are three kinds of Feynman diagrams: Fig. 1(a)–1(c) for the final states $Z_1 Z_1$. Obviously, the amplitude of Fig. 1(b) is suppressed by a factor of $\kappa/\sqrt{s}$ compared with the first one. Thus we only consider the contribution from Fig. 1(a) and 1(c). The total annihilation cross section is found to be

$$\omega_{Z_1 Z_1} \approx \frac{2e^4 \csc^4 2\theta_W}{\pi}\left[1 + \frac{4m^2}{s} - \frac{8m^2(s - 2m^2)}{s^2} y(x_1)\right], \tag{24}$$

where the function $y(x_1)$ is defined by $y(x_1) \equiv \operatorname{arctanh}(x_1)/x_1$ and $x_1 = \sqrt{1 - 4m^2/s}$. Then, we can derive $(m\sigma_0)_{Z_1 Z_1} \le 2.1 \times 10^{-5}\ \mathrm{GeV}^{-1}$ for $m \ge 500$ GeV. It is obvious that this result is not so large as to satisfy the requirement of Eq. (20).

According to the $Z_1 Z_1$ experience, we also calculate the other processes. The corresponding cross sections are given by

$$\omega_{W_1 W_1} \approx \frac{e^4}{32\pi \sin^4\theta_W}\left[3 + \frac{28m^2}{s} - 32\frac{m^2}{s} y(x_1)\right]; \tag{25}$$

$$\omega_{W_2 W_2} \approx \frac{e^4}{128\pi \sin^4\theta_W}\left(1 - \frac{4m_{W_2}^2}{s}\right)^{1/2}\left[\frac{4}{3}\frac{\sin^4\theta_W}{\cos^2 2\theta_W} \times \frac{(s - 4m^2)(s - 4m_{W_2}^2)}{(s - m_{Z_2}^2)^2}\left(1 + \frac{20m_{W_2}^2}{s} + 12\frac{m_{W_2}^4}{s^2}\right) + \left(\frac{\rho_3 v_R^2}{m_{W_2}^2}\right)^2 \frac{s^2 - 4m_{W_2}^2 s + 12m_{W_2}^4}{(s - m_{H_2^0}^2)^2}\right]; \tag{26}$$

$$\omega_{Z_1 Z_2} \approx \frac{e^4 \sec^4\theta_W}{4\pi \cos 2\theta_W}\left(1 - \frac{m_{Z_2}^2}{s}\right)\frac{s^2 - 3m_{Z_2}^2 s + m_{Z_2}^4 + 4m^2 s - 2(s - 2m^2)(4m^2 - m_{Z_2}^2) y(x_1)}{(s - m_{Z_2}^2)^2}; \tag{27}$$

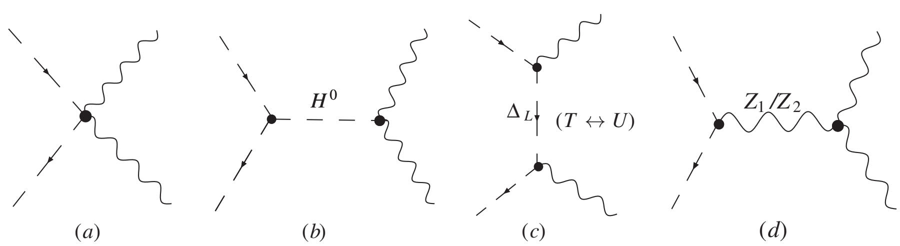

FIG. 1. All possible Feynman diagrams for the annihilation processes $\delta_L^0 \delta_L^{0*} \to VV$, where Δ_L may be $\delta_L^{0/0*}$ or $\delta_L^{\pm}$, and H^0 denotes h^0, H_1^0, and H_2^0.

$$\omega_{Z_2Z_2} \approx \frac{e^4\tan^4\theta_W}{32\pi\cos^2 2\theta_W}\left(1-\frac{4m_{Z_2}^2}{s}\right)^{1/2}\left[4+\frac{(4m^2-m_{Z_2}^2)^2}{m^2 s-4m^2m_{Z_2}^2+m_{Z_2}^4}-4x_\rho\left[2+\frac{8m^2-s-2m_{Z_2}^2}{s-2m_{Z_2}^2}y(x_2)\right]\right.$$
$$\left.-\frac{16(2m^2-m_{Z_2}^2)s-4m^2(16m^2-7m_{Z_2}^2)}{(s-2m_{Z_2}^2)^2}y(x_2)+\left(6-\frac{2s}{m_{Z_2}^2}+\frac{s^2}{2m_{Z_2}^4}\right)x_\rho^2\right], \tag{28}$$

where $x_\rho = (\cot^4\theta_w \rho_3 v_R^2)/(s-m_{H_2^0}^2)$ and $x_2 \equiv \sqrt{(s-4m^2)(s-4m_{Z_2}^2)}/(s-2m_{Z_2}^2)$. These cross sections have the same order as the Z_1Z_1 case. However, the thermally averaged annihilation cross sections of these processes (except for W_1W_1) are far less than the Z_1Z_1 case with $m = 500$ GeV. Therefore, we do not analyze these processes in detail.

C. $\delta_L^0\delta_L^{0*} \to HH/VH$

Let us now focus on the processes $\delta_L^0\delta_L^{0*} \to HH/VH$. The relevant Feynman diagrams for HH and HV are shown in Figs. 2 and 3, respectively. Since the dimensional scalar trilinear couplings enter extensively into the above two annihilation processes, the electroweak scale coupling $\alpha_1\kappa$ in $\delta_L^0\delta_L^{0*}h^0$ and the right-handed scale coupling $\rho_3 v_R$ in $\delta_L^0\delta_L^{0*}H_2^0$ would make a big difference in the $\delta_L^0\delta_L^{0*} \to HV$ processes according to our current parameter setting. Considering the complexity of this model, we only calculate the annihilation cross sections up to leading order (LO) by omitting the next to leading order (NLO) contributions in terms of the following three suppressing factors: (1) small VEV ratio κ/v_R and $\kappa/\sqrt{s}$ due to the big hierarchy in the symmetry breaking scale of the LR model. Since we have made the approximation $\kappa^2/v_R^2 \simeq 0$ thus here it is, of course, a reasonable power counting rule to pick out the LO processes against the NLO ones; (2) gauge coupling suppression e^2; (3) p-wave factor $1-4m^2/s$ due to large suppression in the integration of initial energy of the dark matter pair.

In this subsection, we apply the above three suppressing factors to make an explicit demonstration of the LO processes, then give the convincing dark matter annihilation cross sections. The LO amplitude for each possible annihilation process is listed in Table II. The notations are as follows: $p_{1,2}$ denotes the momentum of the dark matter pair, while $p_{3,4}$ is the momentum of the final states, ϵ is the polar vector of gauge boson:

$$P_{Z_{1,2}} = \frac{(p_1-p_2)\cdot(p_4-p_3)}{s-m_{Z_{1,2}}^2}; \qquad P_{43}^{h,H} = \frac{p_4\cdot\epsilon(p_3)}{s-m_{h^0,H_1^0}^2};$$
$$P_{TU} = \frac{p_2\cdot\epsilon(p_3)}{t-m^2} - \frac{p_1\cdot\epsilon(p_3)}{u-m^2}. \tag{29}$$

Here we only consider the cross sections with amplitude order 1. In terms of Table II, nine LO annihilation cross sections are listed in Table III, where $A = 1-\frac{2(\rho_1+2\rho_2)}{s-2\rho_1 v_R^2}$ and $B = \frac{32\rho_4^2}{\rho_3}\frac{v_R^2}{s-2m_{\delta_R^{\pm\pm}}^2}y(x_3) + \frac{64\rho_4^4}{\rho_3^2}\frac{v_R^4}{sm^2-4m^2m_{\delta_R^{\pm\pm}}^2+m_{\delta_R^{\pm\pm}}^4}$ with

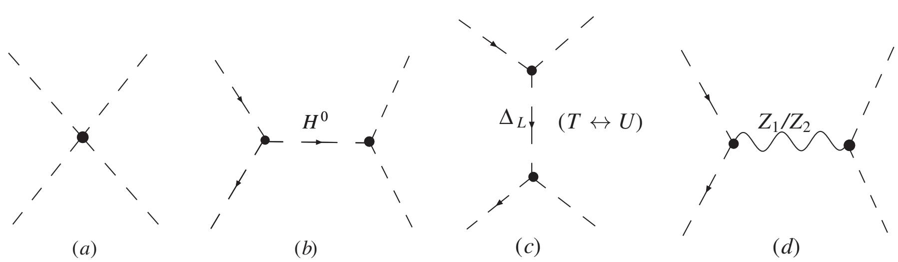

FIG. 2. All possible Feynman diagrams for the annihilation processes $\delta_L^0\delta_L^{0*} \to HH$.

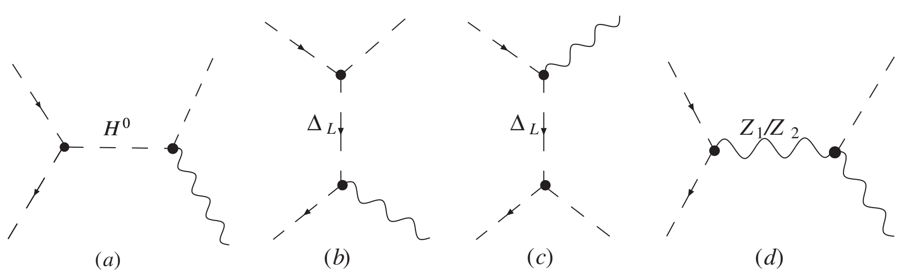

FIG. 3. All possible Feynman diagrams are shown for the annihilation processes $\delta_L^0\delta_L^{0*} \to VH$. The first diagram only appears in the process $\delta_L^0\delta_L^{0*} \to VA_1^0$.

TABLE II. The amplitude for HH/HV final states, where $c_W = \cos\theta_W$, $t_W = \tan\theta_W$, etc. We also estimate the order of corresponding annihilation cross sections.

Process	Amplitude	Order	Process	Amplitude	Order
h^0h^0	$i\alpha_1(1-\frac{\rho_3 v_R^2}{s-2\rho_1 v_R^2})$	1	h^0Z_1	$4ie\alpha_1 \csc 2\theta_W \kappa P_{TU}$	$\frac{e^2}{x_f}\frac{\kappa^2}{s}$
$h^0H_1^0$	$2i\alpha_2(1-\frac{\rho_3 v_R^2}{s-2\rho_1 v_R^2})$	1	$h^0Z_2^0$	$2ie\alpha_1 \frac{t_W}{\sqrt{c_{2W}}}\kappa P_{TU}$	$\frac{e^2}{x_f}\frac{\kappa^2}{s}$
$H_1^0H_1^0$	$i(\alpha_1+\alpha_3)(1-\frac{\rho_3 v_R^2}{s-2\rho_1 v_R^2})$	1	$H_1^0Z_1$	$8ie\alpha_2 \csc_{2W}\kappa P_{TU}$	$\frac{e^2}{x_f}\frac{\kappa^2}{s}$
$A_1^0A_1^0$	$i(\alpha_1+\alpha_3)(1-\frac{\rho_3 v_R^2}{s-2\rho_1 v_R^2})$	1	$H_1^0Z_2$	$4ie\alpha_2 \frac{t_W}{\sqrt{c_{2W}}}\kappa P_{TU}$	$\frac{e^2}{x_f}\frac{\kappa^2}{s}$
$A_1^0H_1^0$	$et_W[c_{2W}P_{Z_1} - t_W P_{Z_2}/2]$	$\frac{e^2}{x_f}$	$A_1^0Z_1$	$4ie\alpha_2 \csc_{2W}\kappa P_{43}^H$	1
$H_2^0H_2^0$	$i\rho_3(2-\frac{6\rho_1 v_R^2}{s-2\rho_1 v_R^2}-\frac{\rho_3 v_R^2}{t-m^2}-\frac{\rho_3 v_R^2}{u-m^2})$	1	$A_1^0Z_2$	$-4ie\alpha_2 \csc_{2W}\sqrt{c_{2W}}\kappa P_{43}^H$	$(\frac{\kappa}{v_R})^2$
$h^0H_2^0$	$-i\rho_3\alpha_1\kappa v_R(\frac{1}{s-2\rho_1 v_R^2}+\frac{1}{t-m^2}+\frac{1}{u-m^2})$	$(\frac{\kappa}{v_R})^2$	$H_2^0Z_1$	$4ie\rho_3 \csc_{2W} v_R P_{TU}$	$\frac{e^2}{x_f}$
$H_1^0H_2^0$	$-2i\rho_3\alpha_2\kappa v_R(\frac{1}{s-2\rho_1 v_R^2}+\frac{1}{t-m^2}+\frac{1}{u-m^2})$	$(\frac{\kappa}{v_R})^2$	$H_2^0Z_2$	$2ie\rho_3 \frac{t_W}{\sqrt{c_{2W}}} v_R P_{TU}$	$\frac{e^2}{x_f}$
$H_1^+H_1^-$	$i\alpha_1[1-(1+\frac{\alpha_3}{\alpha_1})\frac{\rho_3 v_R^2}{s-2\rho_1 v_R^2}]$	1	$H_1^+W_1^-$	$-2ie\alpha_2 \csc_{2W}\kappa P_{43}^H$	1
$\delta_R^{++}\delta_R^{--}$	$i\rho_3[1-\frac{2(\rho_1+2\rho_2)v_R^2}{s-2\rho_1 v_R^2}-\frac{\rho_4}{\rho_3}\frac{8\rho_4 v_R^2}{t-m^2}]$	1	$H_1^+W_2^-$	$-2ie\alpha_2 \csc_{2W}\kappa P_{43}^h$	$(\frac{\kappa}{v_R})^2$

$x_3 = \sqrt{(s-4m^2)(s-4m^2_{\delta_R^{\pm\pm}})}/(s-2m^2_{\delta_R^{\pm\pm}})$; $a = 2 - \frac{3m^2_{H_2^0}}{s-m^2_{H_2^0}}$, $b = 4m^2 + m^2_{H_2^0}$, $c = s - 2m^2_{H_2^0}$, $d = \sqrt{sm^2 - 4m^2 m^2_{H_2^0} + m^4_{H_2^0}}$, and $x_4 = \sqrt{(s-4m^2)(s-4m^2_{H_2^0})}/(s-2m^2_{H_2^0})$. We find that these processes fail to provide enough large cross sections. For $\delta_L^0\delta_L^{0*} \to A_1^0 Z_1$ and $H_1^\pm W_1^\mp$, one can easily obtain $m\sigma_0 \lesssim \alpha_2^2/(16\pi m)$, which is far less than the required lower bound 0.13 GeV^{-1}. Since the other processes have the similar forms, we take the process $\delta_L^0\delta_L^{0*} \to h^0 H_1^0$ as an example to illustrate the main features of this kind of processes. One can immediately derive

$$(m\sigma_0)_{h^0H_1^0} = \frac{\alpha_2^2}{8\pi v_R}\sqrt{\frac{1}{\varepsilon\rho_1} - \frac{1}{4(\varepsilon\rho_1)^2}}\left(\frac{\varepsilon-2}{2\varepsilon-1}\right)^2, \qquad (30)$$

where we have used $\alpha_3 = 2$. It is obvious that the maximum value can be obtained when $\varepsilon\rho_1 = 0.5$. Varying ε, we may derive $(m\sigma_0)_{h^0H_1^0} \lesssim 3.5 \times 10^{-4}$ GeV^{-1} for $\alpha_2 = 2$. Therefore, we do not discuss this class of processes in detail.

D. The resonance case

As pointed out in the previous discussion, the method of calculating the effective thermally averaged annihilation cross section $\langle\sigma_{\rm eff} v\rangle$ is not valid for the resonance case [25]. Here we numerically solve the Boltzmann equation (15), which can be reexpressed as [28]

$$\frac{dY}{dx} = -\frac{x}{H_{x=1}\mathbf{s}(x)}\gamma_{\rm eff}\left(\frac{Y^2}{Y_{\rm eq}^2} - 1\right), \qquad (31)$$

where $H_{x=1}$ is the Hubble parameter evaluated at $T = m$ and $\mathbf{s}(x)$ is the entropy density given by

$$H_{x=1} = \sqrt{\frac{4\pi^3 g_*}{45}}\frac{m^2}{M_{\rm Pl}}, \qquad \mathbf{s}(x) = \frac{2\pi^2 g_*}{45}\frac{m^3}{x^3}. \qquad (32)$$

$Y \equiv n/\mathbf{s}$ is the ratio of the total particle number density n to the entropy density $\mathbf{s}$. The equilibrium number density $Y_{\rm eq}$ reads

$$Y_{\rm eq}(x) = \frac{45}{4\pi^4}\frac{g_{\rm eff}}{g_*}x^2 K_2(x). \qquad (33)$$

In fact, $\gamma_{\rm eff}$ is the reaction density defined by

TABLE III. The annihilation cross sections for the leading order processes.

Process	$4E_1E_2\sigma v$	Process	$4E_1E_2\sigma v$
h^0h^0	$\frac{\alpha_1^2}{16\pi}(1-\frac{\rho_3 v_R^2}{s-2\rho_1 v_R^2})^2$	$H_1^+H_1^-$	$\frac{\alpha_1^2}{8\pi}[1-(1+\frac{\alpha_3}{\alpha_1})\frac{\rho_3 v_R^2}{s-2\rho_1 v_R^2}]^2$
$h^0H_1^0$	$\frac{\alpha_2^2}{2\pi}(1-\frac{m^2_{H_1^0}}{s})^{1/2}(1-\frac{\rho_3 v_R^2}{s-2\rho_1 v_R^2})^2$	$\delta_R^{++}\delta_R^{--}$	$\frac{\rho_3^2}{8\pi}(1-\frac{4m^2_{\delta_R^{\pm\pm}}}{s})^{1/2}(A^2+B)$
$H_1^0H_1^0$	$\frac{(\alpha_1+\alpha_3)^2}{16\pi}(1-\frac{4m^2_{H_1^0}}{s})^{1/2}(1-\frac{\rho_3 v_R^2}{s-2\rho_1 v_R^2})^2$	$A_1^0Z_1$	$\frac{\alpha_2^2}{4\pi}(1-\frac{m^2_{A_1^0}}{s})^{5/2}$
$A_1^0A_1^0$	$\frac{(\alpha_1+\alpha_3)^2}{16\pi}(1-\frac{4m^2_{H_1^0}}{s})^{1/2}(1-\frac{\rho_3 v_R^2}{s-2\rho_1 v_R^2})^2$	$H_1^+W_1^-$	$\frac{\alpha_2^2}{4\pi}(1-\frac{m^2_{H_1^\pm}}{s})^{5/2}$
$H_2^0H_2^0$	$\frac{\rho_3^2}{16\pi}[a^2+\frac{b^2}{2d^2}+\frac{2b}{c}(2a+\frac{b}{c})y(x_4)]$		

TABLE IV. The relic number density $n_{\delta_L^0}$ in terms of different α_1 and ρ_1 for the H_2^0 case.

$\rho_1 = 1.0$	$n_{\delta_L^0}$	$\rho_1 = 0.1$	$n_{\delta_L^0}$
$\alpha_1 = 0.01$	$n_{\delta_L^0} = 6.4 \times 10^{-13}$	$\alpha_1 = 0.01$	$n_{\delta_L^0} = 1.6 \times 10^{-12}$
$\alpha_1 = 0.1$	$n_{\delta_L^0} = 6.5 \times 10^{-13}$	$\alpha_1 = 0.1$	$n_{\delta_L^0} = 1.4 \times 10^{-12}$
$\alpha_1 = 1.0$	$n_{\delta_L^0} = 1.1 \times 10^{-12}$	$\alpha_1 = 1.0$	$n_{\delta_L^0} = 3.6 \times 10^{-12}$
$\alpha_1 = 2.0$	$n_{\delta_L^0} = 2.5 \times 10^{-12}$	$\alpha_1 = 2.0$	$n_{\delta_L^0} = 1.2 \times 10^{-11}$

$$\gamma_{\mathrm{eff}} \equiv n_{\mathrm{eq}}^2 \langle \sigma_{\mathrm{eff}} v \rangle = \frac{m^4}{64\pi^4 x} \int_4^\infty \hat{\sigma}_{\mathrm{eff}}(z)\sqrt{z} K_1(x\sqrt{z}) dz, \tag{34}$$

with

$$\hat{\sigma}_{\mathrm{eff}} = g_{\mathrm{eff}}^2 4E_1 E_2 \sigma_{\mathrm{eff}} v \sqrt{1 - 4/z}, \tag{35}$$

where $z = s/m^2$, $K_1(x)$, and $K_2(x)$ are the modified Bessel functions.

In our scenario, the exchanged particles may be Z_1, Z_2, h^0, H_1^0, and H_2^0. It is obvious that the case of exchanging gauge bosons Z_1 or Z_2 is a p-wave annihilation process. If the exchanged particle is H_1^0, the corresponding cross section will be suppressed by κ^2/v_R^2. For the h^0 case, the resonant condition $2m \approx m_{h^0}$ implies that the final states must be the Fermi pairs. In addition, the previous analysis indicates that the maximal cross section might be from the H_2^0 exchanging process. Therefore, we study the h^0 and H_2^0 cases in this subsection.

First we consider the H_2^0 case. Because of the factor $\sqrt{1 - 4/z}$ in Eq. (35), we take $m_{H_2^0}^2/m^2 = 4.1$ (namely $\varepsilon = 0.4878$). At this point, γ_{eff} becomes larger than the $m_{H_2^0}^2/m^2 = 4$ case. Then we take $\rho_1 = 1$ ($\rho_3 = 2.98$). At this moment, δ_L^0 and δ_L^{0*} may annihilate into h^0h^0, $h^0H_1^0$, and W_2W_2. Since h^0h^0 and $h^0H_1^0$ have a similar form, the key quantity is $\alpha_2^2 + \alpha_1^2/8$ for our calculation. Without loss of generality, one may take different values for α_1 and require $\alpha_1 = \alpha_2$. The final results for different α_1 have been shown in Table IV. In addition, we also calculate the $\rho_1 = 0.1$ case, and list the corresponding results in Table IV. If $\rho_1 = 0.1$, the final states have to be two SM Higgs bosons. In view of Table IV, we may find that the H_2^0 case fails to suppress the relic number density of δ_L^0 and δ_L^{0*}.

Now we assume the SM Higgs mass $m_{h^0} = 120$ GeV in the h^0 case. Furthermore, one may obtain $m = 59.3$ GeV ($\varepsilon\rho_1 = 3.5 \times 10^{-5}$) from $m_{H_2^0}^2/m^2 = 4.1$. Because of $m < 100$ GeV, the bound in Eq. (14) is not valid. For $m = 59.3$ GeV, we take $\sigma_n^{\mathrm{exp}} \leq 4.6 \times 10^{-44}$ cm^2 [16] and derive the corresponding bound

$$n_{\delta_L^0} \leq 1.1 \times 10^{-13}. \tag{36}$$

In this case, δ_L^0 and δ_L^{0*} mainly annihilate into the bottom quark pair. The annihilation cross section is given by

$$(4E_1 E_2 \sigma v)_{h^0} \simeq \frac{3}{4\pi} \frac{\alpha_1^2 m_b^2 s}{(s - m_{h^0}^2)^2 + m_{h^0}^2 \Gamma_{h^0}^2}, \tag{37}$$

where m_b is the bottom quark mass and $\Gamma_{h^0} \simeq 3m_{h^0} m_b^2/(8\pi\kappa^2)$ is the decay width of h^0. One may obtain $n_{\delta_L^0} = 1.2 \times 10^{-15}$ for $\alpha_1 = 2$. This wonderful result indicates that our scenario may be consistent with the direct dark matter search bound. To illustrate, we plot the relic number density $n_{\delta_L^0}$ versus the dark matter mass m in Fig. 4, where all annihilation channels have been considered. Using the results from CERN LEP-II, Datta and Raychaudhuri have derived $m \geq 55.4$ GeV [29]. To show the h^0 resonance region, we choose 48 GeV $\leq m \leq$ 72 GeV ($0.8 \leq 2m/m_{h^0} \leq 1.2$) in Fig. 4. The peak around $2m/m_{h^0} = 0.83$ in Fig. 4 is due to the competition between h^0 and Z_1 resonances. For $m_{h^0} = 120$ GeV, we find that 56 GeV $\lesssim m \lesssim$ 60 GeV can satisfy the requirement $n_{\delta_L^0} \leq 1.1 \times 10^{-13}$. At this moment, one may obtain $\Omega_{\delta_L^0} h^2 \lesssim 6.3 \times 10^{-7}$, which is far less than the total dark matter density $\Omega_{\mathrm{DM}} h^2 = 0.111 \pm 0.006$ [18].

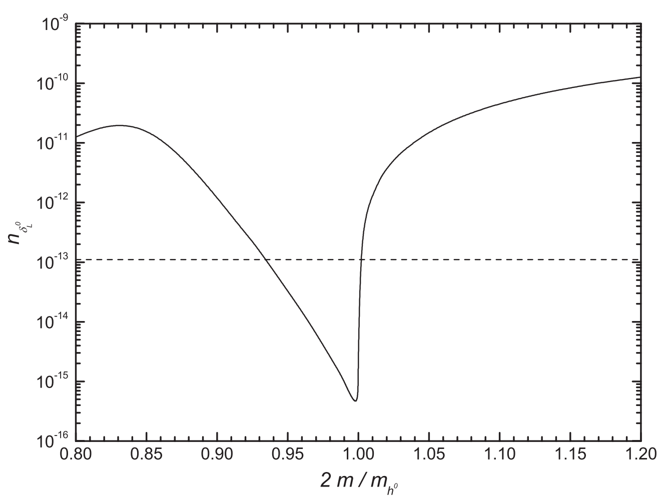

FIG. 4. Numerical illustration of the relic number density $n_{\delta_L^0}$ as a function of $2m/m_{h^0}$ near a resonance, where $m_{h^0} = 120$ GeV has typically been taken. The dashed line denotes the present experimental upper bound on $n_{\delta_L^0}$.

VI. TWO HIGGS BIDOUBLET MODEL

Motivated by the general two Higgs doublet model as a model for spontaneous CP violation, one may simply extend the one Higgs bidoublet LR model to a two Higgs bidoublet LR model with spontaneous P and CP violation [13]. Besides one left-handed Higgs triplet Δ_L (3, 1, 2) and one right-handed Higgs triplet Δ_R (1,3,2), this model consists of two Higgs bidoublets ϕ (2, 2, 0) and χ (2, 2, 0), which can be written as

$$\phi = \begin{pmatrix} \phi_1^0 & \phi_1^+ \\ \phi_2^- & \phi_2^0 \end{pmatrix}; \qquad \chi = \begin{pmatrix} \chi_1^0 & \chi_1^+ \\ \chi_2^- & \chi_2^0 \end{pmatrix}. \tag{38}$$

The most general Yukawa interaction for quarks is given by

$$-\mathcal{L}_Y = \bar{Q}_L(Y_q\phi + \tilde{Y}_q\tilde{\phi} + F_q\chi + \tilde{F}_q\tilde{\chi})Q_R, \tag{39}$$

where $Q_{L,R} = (u_{L,R}, d_{L,R})^T$. Parity P symmetry requires Y_q, $\tilde{Y}_q$, F_q, and $\tilde{F}_q$ are Hermitian matrices. When both P and CP are required to be broken down spontaneously, all the Yukawa coupling matrices are real symmetric. After the spontaneous symmetry breaking, two Higgs bidoublets can have the following vacuum expectation values:

$$\begin{aligned} \langle\phi\rangle &= \begin{pmatrix} \kappa_1/\sqrt{2} & 0 \\ 0 & \kappa_2/\sqrt{2} \end{pmatrix}; \\ \langle\chi\rangle &= \begin{pmatrix} w_1/\sqrt{2} & 0 \\ 0 & w_2/\sqrt{2} \end{pmatrix}, \end{aligned} \tag{40}$$

where κ_1, κ_2, w_1, and w_2 are in general complex. Then we may obtain the following quark mass matrices:

$$\begin{aligned} M_u &= \tfrac{1}{\sqrt{2}}(Y_q\kappa_1 + \tilde{Y}_q\kappa_2 + F_qw_1 + \tilde{F}_qw_2); \\ M_d &= \tfrac{1}{\sqrt{2}}(Y_q\kappa_2 + \tilde{Y}_q\kappa_1 + F_qw_2 + \tilde{F}_qw_1). \end{aligned} \tag{41}$$

In the two Higgs bidoublet model, the stringent constraints from the low energy phenomenology can be significantly relaxed. In Ref. [13], the authors calculate the constraints from the neural K meson mass difference Δm_K and demonstrate that a right-handed gauge boson W_2 contribution in box diagrams with mass around 600 GeV is allowed due to a cancellation caused by a light charged Higgs boson with a mass range 150–300 GeV. Therefore, we take $v_R \approx 2$ TeV instead of the previous $v_R = 10$ TeV for this section. It is worthwhile to stress that our previous estimation is still right for this case except for the process $\delta_L^0\delta_L^{0*} \to h^0H_1^0$. $(m\sigma_0)_{h^0H_1^0}$ in Eq. (30) will be about 5 times larger than that in the $v_R = 10$ TeV case, which does not affect our conclusion.

Since there are two Higgs bidoublets, we can give more dark matter annihilation processes for $\delta_L^0\delta_L^{0*} \to HH$ and $\delta_L^0\delta_L^{0*} \to VH$. In this model, one may obtain three light neutral Higgs bosons and a pair of light charged Higgs bosons [30]. The other Higgs bosons' masses are related to v_R. Although the annihilation cross section might be doubled or even increased by several times, it is still at least 10 times less than the direct dark matter search bound.

A significant advantage of the two Higgs bidoublet model is that the Yukawa couplings may become very large. In view of Eq. (41), one can explicitly understand this feature. For example, we require the couplings Y_q and $\tilde{Y}_q$ are very large when $w_1 \gg \kappa_1 \gg \kappa_2 \approx w_2$. Then one may obtain larger annihilation cross section for the $\delta_L^0\delta_L^{0*} \to f\bar{f}$ process than Eq. (23). For illustration, we take the maximal annihilation cross section for each quark pair final states

$$4E_1E_2\sigma v \sim \frac{3}{8\pi}\frac{(\alpha_iY_qw_1)^2s}{(s - m_h^2)^2}, \tag{42}$$

where m_h denotes the mass of a light Higgs boson which comes from ϕ_1^0. For $\alpha_i = 1$, $w_1 \approx 246$ GeV, and $m = 100$ GeV, $Y_q \gtrsim 4.3$ can be obtained from Eq. (20) when we take $2m/m_h = 0.8$ and consider all quark final states but the top quark. At this moment, we must consider the light Higgs h contribution to the direct dark matter detection experiments. The WIMP-nucleon cross section by exchanging h is given by

$$\sigma_n = \frac{M^2(n)}{2\pi}\left(\frac{\alpha_i}{mm_h^2}\right)^2 f^2M_n^2, \tag{43}$$

where $f \sim 0.02Y_qw_1/m_u$ [15]. Using the above parameter setting, we may derive $\sigma_n \gtrsim 6.1 \times 10^{-35}$ cm^2, which is far more than the Z_1 exchanging case of Eq. (13). The larger Y_q is, the larger σ_n is. Therefore, we cannot give the desired relic number density through increasing the Yukawa couplings.

Now we focus on the resonance case. For the H_2^0 exchanging case, the results in Table IV can be increased by about 5 times because of $v_R \approx 2$ TeV. On the other hand, more final states would generally increase the partial width $\Gamma_{H_2^0\to HH}$. Namely the case of more final states is equivalent to enhancing α_1, which does no good for the larger annihilation cross section as shown in Table IV. For the h^0 case, we may obtain the same conclusion as the one Higgs bidoublet case.

VII. SUMMARY AND COMMENTS

In the left-right symmetric model with one Higgs bidoublet, we have demonstrated that the cold dark matter constraints should be considered in a specific scenario in which the so-called VEV-seesaw problem can be naturally solved. In such a scenario, we find that δ_L^0 and δ_L^{0*} are two degenerate and stable particles. To avoid the conflict with the direct dark matter detection experiments, we obtain the relic number density $n_{\delta_L^0} \leq 4.8 \times 10^{-14}$, which implies that the two particles cannot dominate all the dark matter. Subsequently, the lower bounds $m\sigma_0 \geq 0.13$ GeV^{-1} and $m\sigma_0 \geq 9.8$ GeV^{-1} have been derived for the s-wave annihilation and the p-wave annihilation, respectively. In this paper, we examine whether our scenario can provide very large annihilation cross sections so as to give the desired relic abundance. We analyze in detail four classes of annihilation processes: $\delta_L^0\delta_L^{0*} \to f\bar{f}$, $\delta_L^0\delta_L^{0*} \to VV$,

$\delta_L^0\delta_L^{0*} \to HH$, and $\delta_L^0\delta_L^{0*} \to VH$. However, our analysis shows that this scenario fails to suppress the relic number density of δ_L^0 and δ_L^{0*} except for the resonance case [31]. For the h^0 resonance case, we obtain $\Omega_{\delta_L^0} h^2 \lesssim 6.3 \times 10^{-7}$, which is far less than the total dark matter density $\Omega_{\rm DM}h^2 = 0.111 \pm 0.006$. Finally, we discuss the two Higgs bidoublet model from the following three aspects: (1) $v_R \approx 2$ TeV; (2) more final states; (3) large Yukawa couplings. It turns out that our previous conclusions can be generalized to the two Higgs bidoublet model.

In recent years, several authors have shown that it is far from natural for the minimal LR model to generate spontaneous CP violation with natural-sized Higgs potential parameters [3–5]. It is of importance for us to comment on some more general LR models with one Higgs bidoublet [6–11]. The differences mainly come from the complexity of the Higgs potential parameter α_2 and Yukawa couplings. We stress that our conclusion in Sec. V could be generalized to these more general cases without any dramatic alternation because the gauge and Higgs sectors are basically the same.

ACKNOWLEDGMENTS

This work was supported by the National Nature Science Foundation of China (NSFC) under the Grant No. 10475105 and No. 10491306. W. L. Guo is supported by the China Postdoctoral Science Foundation and the K. C. Wong Education Foundation (Hong Kong).

APPENDIX: SCALAR AND SCALAR-GAUGE TRILINEAR AND QUARTIC COUPLINGS

We intend to calculate the cross section to the leading order for each process of dark matter annihilation. We first work in the framework of the simple left-right symmetric model with one Higgs bidoublet and one pair of LR triplets. To simplify our calculation, we take the decoupling limit in which $\kappa^2/v_R^2 \simeq 0$ where $\kappa^2 = |\kappa_1|^2 + |\kappa_2|^2$ denotes the EWSB scale. The VEVs of the Higgs bidoublet are required to satisfy the low energy phenomenology constraint $\kappa_2/\kappa_1 \leq m_b/m_t$, which may produce correct quark masses, small quark mixing angles, and the suppression of flavor-changing neutral currents [32–35]. For simplicity, we take $\kappa_2 \simeq 0$ which is a reasonable approximation at the leading order since κ_2/κ_1 is now around 10^{-2}. Actually the limit $\kappa_2 \to 0$ brings an additional advantage that the vacuum CP phase θ_2 could be taken zero safely without hampering the estimation. These approximations could largely simplify our calculation.

The relevant scalar trilinear couplings and quartic couplings under the unitary gauge are shown in Table V. Here we write out the scalar-gauge interactions:

$$\mathcal{L}_{\delta_L^0\delta_L^{0*}VV} = \delta_L^0\delta_L^{0*}(gW_{3L} - g'B)^2 + g^2\delta_L^0\delta_L^{0*}W_L^+W_L^-; \tag{A1}$$

$$\mathcal{L}_{\delta_L^0\delta_L V} = -ig(\delta_L^0\partial\delta_L^- - \delta_L^-\partial\delta_L^0)W_L^+ + i\delta_0\partial\delta_L^{0*}(gW_{3L} - g'B) + \text{H.c.}; \tag{A2}$$

$$\begin{aligned}\mathcal{L}_{HVV} = {}& g^2 v_R\Big\{H_2^0[(gW_{3R} - g'B)(gW_{3R} - g'B) + W_R^+W_R^-] + \Big(-\frac{1}{\sqrt{2}}\delta_R^{--}W_R^+W_R^+ + \text{H.c.}\Big)\Big\} \\ & + g^2 k\Big\{\frac{1}{2}H_1^-(W_{3R}W_L^+ - W_{3L}W_R^+) - \frac{1}{2}(H_1^0 + iA_1^0)W_L^-W_R^+ + \text{H.c.} + \frac{1}{4}h^0[(W_{3L} - W_{3R})(W_{3L} - W_{3R}) \\ & + 2(W_L^+W_L^- + W_R^+W_R^-)]\Big\};\end{aligned} \tag{A3}$$

TABLE V. The relevant trilinear and quartic scalar couplings, where the dimensional trilinear couplings with different scales v_R and κ are separated and shown separately in two columns: $\tilde{\lambda} = \lambda_1 + 4\lambda_2 + 2\lambda_3$ and $\tilde{\lambda}' = \lambda_1 - 4\lambda_2 + 2\lambda_3$.

Interaction	Coupling/v_R	Interaction	Coupling/κ	Interaction	Coupling
$\delta_L^0\delta_L^{0*}H_2^0$	ρ_3	$\delta_L^0\delta_L^{0*}h^0$	α_1	$\delta_L^0\delta_L^{0*}h^0h^0$	α_1
$\delta_L^0\delta_L^{--}\delta_R^{++}$	$2\sqrt{2}\rho_4$	$\delta_L^0\delta_L^{0*}H_1^0$	$2\alpha_2$	$\delta_L^0\delta_L^{0*}h^0H_1^0$	$2\alpha_2$
$H_2^0h^0h^0$	α_1	$h^0h^0h^0$	$6\lambda_1$	$\delta_L^0\delta_L^{0*}H_1^0H_1^0$	$\alpha_1+\alpha_3$
$H_2^0H_1^0h^0$	$2\alpha_2$	$H_1^0h^0h^0$	$6\lambda_4$	$\delta_L^0\delta_L^{0*}A_1^0A_1^0$	$\alpha_1+\alpha_3$
$H_2^0H_1^0H_1^0$	$\alpha_1+\alpha_3$	$H_1^0H_1^0h^0$	$2\tilde{\lambda}$	$\delta_L^0\delta_L^{0*}H_1^+H_1^-$	α_1
$H_2^0A_1^0A_1^0$	$\alpha_1+\alpha_3$	$H_1^0H_1^0H_1^0$	$6\lambda_4$	$\delta_L^0\delta_L^{0*}H_2^0H_2^0$	$2\rho_3$
$H_2^0H_1^+H_1^-$	$\alpha_1+\alpha_3$	$H_1^0A_1^0H_1^0$	$2\lambda_4$	$\delta_L^0\delta_L^{0*}\delta_R^{++}\delta_R^{--}$	ρ_3
$H_2^0H_2^0H_2^0$	$6\rho_1$	$h^0A_1^0A_1^0$	$2\tilde{\lambda}'$		
$H_2^0\delta_R^{++}\delta_R^{--}$	$2(\rho_1+2\rho_2)$	$H_2^0H_2^0h^0$	α_1		
		$H_2^0H_2^0H_1^0$	$2\alpha_2$		

$$\mathcal{L}_{HHV} = \frac{ig}{2}H_1^- \partial H_1^+ (W_{3L} + W_{3R}) - i\delta_R^{++}\partial\delta_R^{--}(gW_{3R} + g'B) - ig(\delta_R^{--}\partial\delta_R^{+} - \delta_R^{+}\partial\delta_R^{--})W_R^+ + \frac{ig}{2}[(H_1^-\partial H_1^0 - H_1^0\partial H_1^-)W_L^+ + (h^0\partial H_1^- - H_1^-\partial h^0)W_R^+] + \frac{g}{2}[(A_1^0\partial H_1^- - H_1^-\partial A_1^0)W_R^+ + h.c. + (H_1^0\partial A_1^0 - A_1^0\partial H_1^0)(W_{3L} - W_{3R})], \tag{A4}$$

where the connection between weak eigenstates (W_{3L}, W_{3R}, B) and physical states (Z_1, Z_2, A) are demonstrated by the following orthogonal transformation at the leading order:

$$\begin{pmatrix} W_{3L} \\ W_{3R} \\ B \end{pmatrix} = \begin{pmatrix} c_W & 0 & s_W \\ -s_W t_W & \sqrt{c_{2W}}\sec_W & s_W \\ -\sqrt{c_{2W}}t_W & -t_W & \sqrt{c_{2W}} \end{pmatrix}\begin{pmatrix} Z_1 \\ Z_2 \\ A \end{pmatrix}. \tag{A5}$$

The $SU(2)_{L,R}$ gauge coupling g and $U(1)_{B-L}$ coupling g' are related to the $U(1)_{\rm EM}$ gauge coupling e:

$$g = \frac{e}{\sin\theta_W}, \qquad g' = \frac{e}{\sqrt{\cos 2\theta_W}}. \tag{A6}$$

Here our conventions are the same as those in Ref. [20].

[1] J. C. Pati and A. Salam, Phys. Rev. D **10**, 275 (1974); R. N. Mohapatra and J. C. Pati, Phys. Rev. D **11**, 566 (1975); G. Senjanovic and R. N. Mohapatra, Phys. Rev. D **12**, 1502 (1975).
[2] T. D. Lee, Phys. Rev. D **8**, 1226 (1973); Phys. Rep. **9**, 143 (1974).
[3] A. Masiero, R. N. Mohapatra, and R. D. Peccei, Nucl. Phys. **B192**, 66 (1981); J. Basecq, J. Liu, J. Milutinovic, and L. Wolfenstein, Nucl. Phys. **B272**, 145 (1986).
[4] N. G. Deshpande, J. F. Gunion, B. Kayser, and F. Olness, Phys. Rev. D **44**, 837 (1991).
[5] G. Barenboim, M. Gorbahn, U. Nierste, and M. Raidal, Phys. Rev. D **65**, 095003 (2002); Y. Rodriguez and C. Quimbay, Nucl. Phys. **B637**, 219 (2002).
[6] P. Langacker and S. U. Sankar, Phys. Rev. D **40**, 1569 (1989).
[7] G. Barenboim, J. Bernabeu, J. Prades, and M. Raidal, Phys. Rev. D **55**, 4213 (1997).
[8] M. E. Pospelov, Phys. Rev. D **56**, 259 (1997).
[9] P. Ball, J. M. Frere, and J. Matias, Nucl. Phys. **B572**, 3 (2000).
[10] K. Kiers, M. Assis, and A. A. Petrov, Phys. Rev. D **71**, 115015 (2005).
[11] Y. Zhang, H. P. An, X. D. Ji, and R. N. Mohapatra, Phys. Rev. D **76**, 091301 (2007); Nucl. Phys. **B802**, 247 (2008).
[12] K. Kiers, J. Kolb, J. Lee, A. Soni, and G. H. Wu, Phys. Rev. D **66**, 095002 (2002).
[13] Y. L. Wu and Y. F. Zhou, arXiv:0709.0042.
[14] P. Minkowski, Phys. Lett. B **67**, 421 (1977); T. Yanagida, in *Proceedings of the Workshop on Unified Theory and the Baryon Number of the Universe*, edited by O. Sawada and A. Sugamoto (KEK, Tsukuba, 1979); M. Gell-Mann, P. Ramond, and R. Slansky, in *Supergravity*, edited by F. van Nieuwenhuizen and D. Freedman (North-Holland, Amsterdam, 1979); S. L. Glashow, in *Quarks and Leptons*, edited by M. Lévy *et al.* (Plenum, New York, 1980); R. N. Mohapatra and G. Senjanovic, Phys. Rev. Lett. **44**, 912 (1980).
[15] For a review, see: G. Jungman, M. Kamionkowski, and K. Griest, Phys. Rep. **267**, 195 (1996); G. Bertone, D. Hooper, and J. Silk, Phys. Rep. **405**, 279 (2005).
[16] CDMS Collaboration, arXiv:0802.3530; CDMS Collaboration, Phys. Rev. Lett. **96**, 011302 (2006).
[17] XENON Collaboration, Phys. Rev. Lett. **100**, 021303 (2008).
[18] W. M. Yao *et al.* (Particle Data Group), J. Phys. G **33**, 1 (2006).
[19] O. Khasanov and G. Perez, Phys. Rev. D **65**, 053007 (2002).
[20] P. Duka, J. Gluza, and M. Zralek, Ann. Phys. (N.Y.) **280**, 336 (2000).
[21] J. D. Lewin and P. F. Smith, Astropart. Phys. **6**, 87 (1996).
[22] M. Cirelli, N. Fornengo, and A. Strumia, Nucl. Phys. **B753**, 178 (2006).
[23] R. Barbieri, L. J. Hall, and V. S. Rychkov, Phys. Rev. D **74**, 015007 (2006); E. M. Dolle and S. F. Su, Phys. Rev. D **77**, 075013 (2008).
[24] J. D. Bekenstein, Phys. Rev. D **70**, 083509 (2004); C. Skordis, D. F. Mota, P. G. Ferreira, and C. Boehm, Phys. Rev. Lett. **96**, 011301 (2006); I. Ferreras, M. Sakellariadou, and M. F. Yusaf, Phys. Rev. Lett. **100**, 031302 (2008); X. F. Wu, B. Famaey, G. Gentile, H. Perets, and H. S. Zhao, arXiv:0803.0977, and references cited therein.
[25] K. Griest and D. Seckel, Phys. Rev. D **43**, 3191 (1991).
[26] E. W. Kolb and M. S. Turner, *The Early Universe* (Addison-Wesley, Reading, MA, 1990).
[27] M. Srednicki, R. Watkins, and K. A. Olive, Nucl. Phys. **B310**, 693 (1988); P. Gondolo and G. Gelmini, Nucl. Phys. **B360**, 145 (1991).

[28] J. Edsjo and P. Gondolo, Phys. Rev. D **56**, 1879 (1997).
[29] A. Datta and A. Raychaudhuri, Phys. Rev. D **62**, 055002 (2000).
[30] Y. J. Huo, L. M. Wang, and Y. L. Wu (unpublished).
[31] It needs to be mentioned that δ_L^0 and δ_L^{0*} may be the candidate of the cold dark matter when we use the MOND to explain the rotation curves of disk galaxies.
[32] G. Ecker, W. Grimus, and W. Konetschny, Phys. Lett. B **94**, 381 (1980); Nucl. Phys. **B177**, 489 (1981).
[33] J. M. Frere, J. Galand, *et al.*, Phys. Rev. D **46**, 337 (1992).
[34] G. Barenboim, J. Bernabeu, and M. Raidal, Nucl. Phys. **B478**, 527 (1996).
[35] P. Ball, arXiv:hep-ph/0004345.